

Current Biology, Volume 21
Supplemental Information

Alternative Sites of Synaptic Plasticity
in Two Homologous “Fan-out Fan-in”

Learning and Memory Networks

T. Shomrat, N. Graindorge, C. Bellanger, G. Fiorito, Y. Loewenstein, B. Hochner

Inventory of Supplemental Information

Figure S1, related to Figure 2

Figure S2, related to Figure 3

Supplemental Experimental Procedures

Supplemental Discussion

Supplemental Computational Considerations

Supplemental References

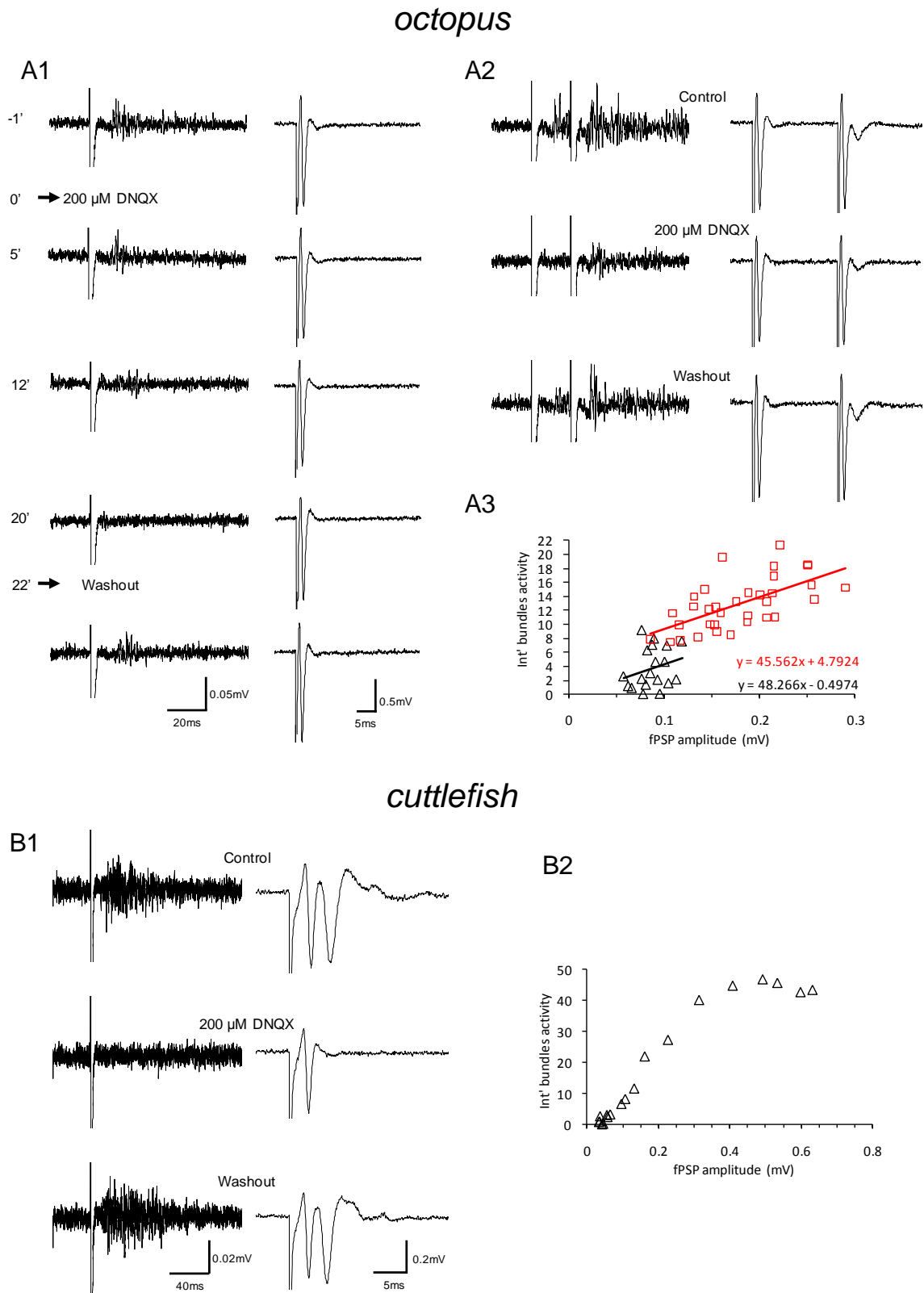


Figure S1. Blocking the glutamatergic fPSP resulted in a correlated blockage of large cell (LN) output, measured as bundle activity, both in octopus (A) and cuttlefish (B). **A1.** Raw

traces of bundle activity (left) and LFP (right) at the times denoted with respect to administration of 200 μ M DNQX. Note the correlation between the fPSP amplitude and bundle activity at various stages of an experiment. This correlation is plotted in A3 (black triangles). **A2.** Similar to A1 but with twin pulse stimulation. Traces are from the control, at the time of maximal effect and after 25 min. of washout. The second stimulus of the pair caused a robust facilitation of both the fPSP and bundle activity. While DNQX completely blocked the responses to the first stimulus (middle traces), the facilitated second fPSP partially overcame the DNQX blockade; as a result bundle activity was also evident. The correlation between the second responses is plotted in A3 (red squares). **A3.** The linear correlation between the fPSP amplitude and the integrated bundle activity (measured at 10 ms time window starting 10 ms after the first or the second stimulus artifact) suggests that the glutamatergic input to the AM determines the input to LN (via the cholinergic AM \rightarrow LN synapse). **B1.** Similar to A1 in cuttlefish. Traces are from control, 12 min after administration of 200 μ M DNQX, and 15 min. after washout. Note the large fPSP and bundle activity evoked by a single stimulus are typical of cuttlefish. **B2.** Correlation between fPSP amplitude and integrated bundle activity in cuttlefish (50 - 130 ms). Note the range of linear relationships at lower fPSP amplitudes and saturation of LN output at the larger fPSP amplitudes.

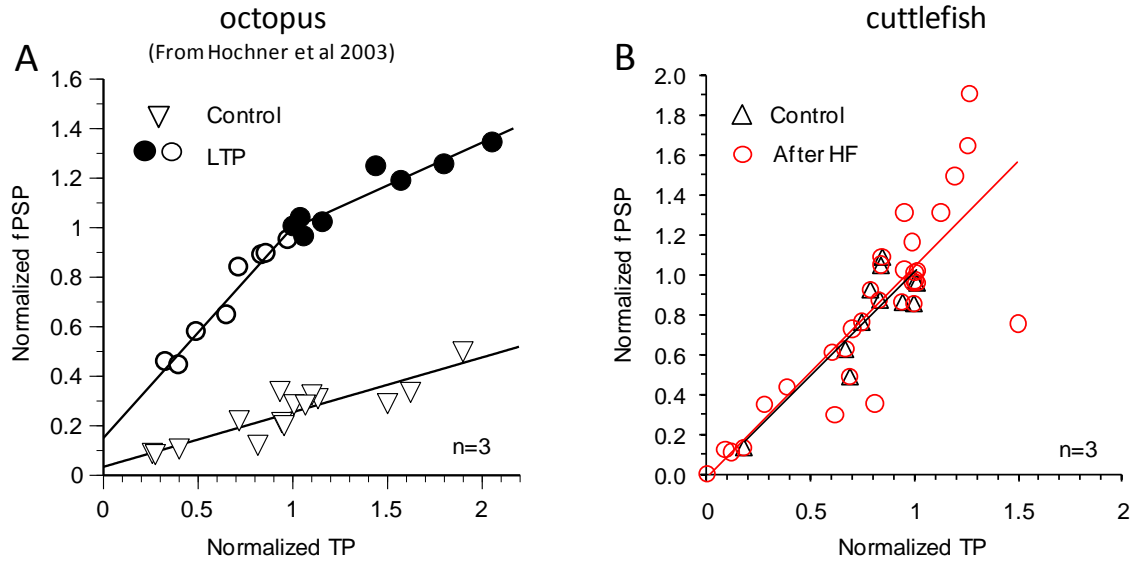


Figure S2. A linear dependence of fPSPs on tract potentials (TP) amplitude is changed dramatically following LTP induction in octopus but not in cuttlefish. (A. octopus (from Hochner et al. 2003), B. cuttlefish). The dependence of fPSP on TP amplitude was examined by varying the intensity of SFL tract stimulation before (open triangles) and after LTP induction by 4XHF tetanizations (empty and filled circles). The fPSP and the TP are normalized to those obtained by a test pulse at the same intensity used for HF stimulation. **A.** The control results are scaled by the average LTP (=4.0). Three regression lines are fitted to the control (triangles, $r = 0.8937$, $p < 0.0001$), after LTP at the range of $TP \leq 1$ (open circles, $r = 0.9754$, $p \leq 0.0015$) and $TP > 1$ (filled circles, $r = 0.9459$, $p \leq 0.0028$). Following LTP, the slope increased only at TP potentials equal to or less than the tetanization amplitude (i.e. $TP \leq 1$). The dependence at higher amplitudes remained close to the pre-LTP slope. This suggests that only the tetanized axons were potentiated (see Hochner et al 2003 for further explanation) **B.** The same procedure as in A. Note the same linear relationships before and after the HF (Control; $r = 0.867$, $p \leq 0.0007$; After HF; $r = 0.84$, $p \leq 0.14 \times 10^{-7}$). The slopes are indistinguishable as expected from the lack of LTP of fPSP in the cuttlefish. (**n** depicts the number of experiments)

Supplemental Experimental Procedures

Experimental animals and maintenance

Mature octopuses (*Octopus vulgaris*) and cuttlefish (*Sepia officinalis*) of both sexes were collected by fishermen from the Israeli and Neapolitan Mediterranean shores. In the Israeli laboratory the cephalopods were held individually in a closed synthetic seawater system. This consisted of aquaria (80-100 liters) with biological and chemical filters maintained at 18°C on a 12h light and dark cycle. In Naples, octopuses were kept individually and cuttlefish in groups of 1-4, in tanks with a running seawater system, also on a 12h light and dark cycle. Once in the laboratory, the animals were acclimatized for at least two weeks before being used for experiments.

Brain slice preparation

Octopuses and cuttlefish were first anesthetized in a bucket with 2L of seawater that was supplemented with an additional 55 mM MgCl₂ and 1% ethanol. This led to a deep anesthesia in the octopuses after ~25–45 min and ~10-20 min in cuttlefish (depending on body weight and water temperature).

Under the dissecting microscope, skin and muscles were removed from the octopus' skull-like cartilaginous cranial structure, which was then cut longitudinally to expose the brain. The thick fluid jelly that surrounds the brain was removed using a sterile syringe and forceps, and the supraesophageal brain mass was carefully removed [1]. The supraesophageal mass was fixed with acrylic glue to a vibratome stage and supported underneath and at the back by agar blocks. To reduce intense injury discharges and synaptic activity during slicing, the vibratome bath was filled with a 70:30% mixture of ASW and an isotonic solution of MgCl₂ (370 mM) at ~4°C. The octopus brain is covered

by a tough fibrous sheath that hinders sectioning. This was therefore removed using fine forceps and scissors. Around six 400 μm sagittal slices could be produced from one brain. The slices were maintained at 15°C in culture medium (L15 with L-glutamine and antibiotics, adjusted to seawater salt concentration). The slices preserved their physiological properties without appearing to deteriorate for up to 5 days but we usually used them for no longer than 3 days after preparation. Physiological experiments started 1½ hr after slice preparation.

Cuttlefish slices were prepared as for octopus. The fibrous sheath covering the brain in cuttlefish is thinner than in the octopus and the fluid around the brain is watery, so these were not removed. Unlike the octopus, the cuttlefish slices could be maintained in better conditions for up to two days in ASW rather than L-15 culture medium. Approximately fifteen 400 μm sagittal slices could be produced from one cuttlefish brain but only ~10 of them were suitable for our experiments, as the SF tract is present only in the lateral parts of the cuttlefish VL.

Solutions and drugs

Artificial seawater (ASW) was used as the physiological extracellular solution. Its composition was (in mM): NaCl, 460; KCL, 10; MgCl₂, 55; CaCl₂, 11; glucose, 10; HEPES, 10; buffered to pH 7.6 with NaOH.

For whole-cell recording pipettes we used an internal solution used for octopus arm muscle cells [2]: (in mM): 465 K-gluconate, 2 MgCl₂, 1 CaCl₂, 10 K-EGTA, 5 Na₂ATP, 0.5 Na₂GTP, and 50 HEPES, buffered to pH 7.2 with KOH.

All drug were obtained from Sigma and given in the following doses: CNQX disodium salt (100-200 μM), DNQX (100-400 μM), kynurenic acid (20mM), 5-HT (serotonin

creatinine sulfate complex) (100-200 μ M), hexamethonium-bromide or chloride (0.1-10mM)

Perfusion and drug administration

A peristaltic pump was used to continuously perfuse the experimental chamber with oxygenated ASW at room temperature at a rate of \sim 3.5 ml/min (\sim 2 volume changes/min). Drugs and experimental solutions were introduced via the perfusion system and took \sim 1-3 min to reach the recording site. All drugs were freshly made before each experiment. If a drug was dissolved in DMSO (dimethyl sulfoxide) the final maximal concentration of DMSO in the experimental solution was 0.1% and this was found to have no physiological effect. When required, pH was readjusted to 7.6.

Physiological experiments

SFL tract stimulation (see scheme and inset Fig. 1C).

The SFL tract was stimulated with ASW-filled glass microelectrodes. The patch micropipettes were carefully broken at the tip to increase tip diameter. A silver wire was wrapped around the outside of the pipette as reference electrode. SFL tract stimulation consisted of 0.2 ms monopolar pulses generated by an isolation unit (ISO-flex, A.M.P.I.). The stimulation and recording (see below) systems were controlled and synchronized by a pulse generator (Master 8, A.M.P.I.).

Extracellular local field potential (LFP) recording

DC-coupled extracellular field potentials were recorded by glass microelectrodes (2-3 M Ω) filled with ASW. Signals were bandpass- filtered between 0.3-10 kHz. The 10x output of the AxoClamp 2B amplifier was further amplified x100 (DP-301, Warner Instruments) and stored on a PC hard disc.

Whole-cell recording (see scheme Fig. 1C)

Differential interference contrast (DIC) optics together with infrared video microscopy (Olympus BX51WI with Corail Intensified CCD Camera, VX45, Optronis) allowed better visualization of single neurons in live brain slices in both octopus and cuttlefish [3]. Combining these methods with the whole-cell recording configuration allowed characterization of the membrane properties and synaptic inputs of LN (dia.~17 μm).

Extracellular recording of activity in LN axon bundles (see scheme in Fig. 1C)

Suction micropipettes (50-100 μm diameter) were used to record activity from bundles of LN axons. Sharp microelectrodes were cut at the tip, fire-polished and filled with ASW. The axon bundles were visible under the dissecting microscope and were gently drawn *en passant* into the suction micropipette. The micropipette was connected to a low-level AC differential amplifier (DP-301, Warner Instruments) and efferent activity was recorded differentially to a silver wire wrapped around the micropipette. The signal was amplified (x10,000) and bandpass-filtered (0.3-10 kHz).

Acquisition of electrophysiological data

A multipurpose amplifier (Axoclamp 2B) was used for whole-cell and LFP recordings. The current and voltage signals were digitized by a National Instruments board (PCI-6014) at 20 kHz and stored on a PC hard disc with a custom-made program written in the LabView environment (V 6.1, National Instruments, Austin TX).

Data analysis

Electrophysiological data were analyzed offline using a custom-built program written in the LabView environment (V 6.1, National Instruments, Austin, TX) and MATLAB (The MathWork, Natick, MA, USA). Excel 2007 (Microsoft Corporation) was used to plot the data and for part of the statistical analysis.

Tract and synaptic field potentials were measured from averages of 3-10 traces of test responses. The amplitude of the TP was measured from the first positive peak to the following negative peak. The fPSP amplitude was measured from the negative peak to maximal positive peak (see Fig. 1D1). fPSPs were scaled to correct for small changes in TP amplitude during the experiments (fPSP/TP). Due to the linear relation between the two (Fig S2, see [4]) this procedure did not introduce a large error

Quantification of the extracellular activity of the LN axon bundles

Activity in the bundles was analyzed using Matlab software. The signal was digitized, rectified and the integrated activity calculated. The level of activity was integrated during a time period starting at the end of stimulus artifact and ending when the activity faded to about its pre-stimulation level. The net evoked activity was calculated by subtracting the integrated activity of a similar time period before the stimulus.

Supplemental Discussion

In developing brains plasticity is often observed in fan-out architectures as we describe here in adults octopuses. A well studied example is the mammalian postembryonic ‘critical period’ during which there is plasticity in the first layer of synaptic input in visual, olfactory and probably also auditory cortices [5-11]. The role of this plasticity in the critical period may be to establish relevant representations of the sensory

environment. The adult octopus may use this plasticity to adapt its internal representation to a new environment, enabling familiarization [12].

Supplemental Computational Considerations

In this section we demonstrate the computational equivalence of plasticity in the SFL→AM connections and in the AM→LN connections, when the AM neurons are linear, in the framework of rate equations.

Simplified models of neuronal networks are often described using rate equations in which the state of a neuron is characterized by a smooth rate variable [13-15]. In these models, the input to a neuron is the linear sum of presynaptic activities whose coefficients are the synaptic weights of the networks. The output of the neuron is a low-pass filter of a function of this input. In this framework, the equations that govern the dynamics of the AM neurons as a function of the SFL neurons are:

$$\tau \frac{dA_i}{dt} = -A_i + F \left(\sum_{j=1}^{N_S} J_{ij} S_j \right) \quad (1)$$

where A_i and S_j are the activities of AM neuron i and SFL neuron j , respectively, N_S is the number of SFL neurons, τ is the time constant of the rate dynamics, J_{ij} is the strength of the synaptic connection from SFL neuron j to AM neuron i and F is the steady-state firing rate of the neuron as a function of its input current (Fig. 1B).

Typically, this input-output function F is non-linear, reflecting the non-linear relation of the steady-state firing rate of neurons to the total synaptic input. Similarly, in machine learning, the function F is non-linear, thus projecting the inputs to a higher dimension

space. However, as described in the text (see also Fig. S2), the AM neurons are inexcitable, and their output is proportional to their input. Formally,

$$F(x) = a \cdot x \quad (2)$$

where a is a parameter. Thus, the transformation from the SFL neurons to the AM neurons is linear and therefore the dimension of the activities of the AM neurons cannot be larger than the dimension of the activity of the SFL neurons. This has profound consequences for the computational capabilities of the network. To show this, we consider the input to the LN neuron k , which we denoted by I_k . This input is a function of the activities of the AM neurons A_i , weighted by the synaptic weights W_{ki} :

$$I_k = \sum_{i=1}^{N_A} W_{ki} A_i \quad (3)$$

where N_A is the number of AM neurons. Substituting Eq. (2) in Eq. (1), solving the differential equations and substituting the solution in Eq. (3) yields:

$$I_k(t) = a e^{-\frac{t}{\tau}} \int_0^t e^{\frac{t'}{\tau}} \sum_j M_{kj} S_j(t') dt' \quad (4)$$

where

$$M_{kj} = \sum_i W_{ki} J_{ij} \quad (5)$$

According to Eq. (5), the dependence of the vector of inputs to the LN neurons \vec{I} on the input activities \vec{S} is mediated by the N_L -by- N_S matrix \mathbf{M} , which is a product of the N_L -by- N_A matrix \mathbf{W} and the N_A -by- N_S matrix \mathbf{J} : $\mathbf{M} = \mathbf{W} \cdot \mathbf{J}$, where N_L is the number of LN neurons.

In this manuscript we show that the difference between the cuttlefish and the octopus VL lies in the locus of the plastic changes in synaptic efficacies. In the framework of the rate equations, the values of the elements of \mathbf{W} in the octopus are fixed, while the values of the elements of \mathbf{J} are plastic. In contrast, in the cuttlefish \mathbf{J} is fixed while \mathbf{W} is plastic. However, in general, any matrix \mathbf{M} can be formed by plastic changes in *either* \mathbf{J} or \mathbf{W} . More precisely, assuming that $N_A \geq \max(N_S, N_L)$, if the rank of \mathbf{J} is N_S , $rk(\mathbf{J}) = N_S$ then for every matrix \mathbf{M} there exists a matrix $\mathbf{W} = \mathbf{M} \cdot (\mathbf{J}^t \cdot \mathbf{J})^{-1} \cdot \mathbf{J}^t$ such that $\mathbf{M} = \mathbf{W} \cdot \mathbf{J}$. Note that the matrix $\mathbf{J}^t \cdot \mathbf{J}$ is invertible if and only if $rk(\mathbf{J}) = N_S$. Similarly, if the rank of \mathbf{W} is N_L , then for every matrix \mathbf{M} there exists a matrix $\mathbf{J} = \mathbf{W}^t \cdot (\mathbf{W} \cdot \mathbf{W}^t)^{-1} \cdot \mathbf{M}$ such that $\mathbf{M} = \mathbf{W} \cdot \mathbf{J}$. Again, the matrix $\mathbf{W} \cdot \mathbf{W}^t$ is invertible if and only if $rk(\mathbf{W}) = N_L$.

Thus, the same computation (\mathbf{M}) can be obtained in the octopus and the cuttlefish independently of the locus of plasticity.

Supplemental References

1. Young, J.Z. (1971). The anatomy of the nervous system of *Octopus vulgaris* (Oxford: Clarendon Press).
2. Rokni, D., and Hochner, B. (2002). Ionic Currents Underlying Fast Action Potentials in the Obliquely Striated Muscle Cells of the Octopus Arm. *J Neurophysiol* 88, 3386-3397.
3. Stuart, G.J., Dodt, H.U., and Sakmann, B. (1993). Patch-clamp recordings from the soma and dendrites of neurons in brain slices using infrared video microscopy. *Pflugers Arch* 423, 511-518.
4. Hochner, B., Brown, E.R., Langella, M., Shomrat, T., and Fiorito, G. (2003). A Learning and Memory Area in the Octopus Brain Manifests a Vertebrate-Like Long-Term Potentiation. *J Neurophysiol* 90, 3547-3554.
5. Feldman, D.E. (2009). Synaptic Mechanisms for Plasticity in Neocortex. *Annual Review of Neuroscience* 32, 33-55.
6. Turrigiano, G.G., and Nelson, S.B. (2004). Homeostatic plasticity in the developing nervous system. *Nat Rev Neurosci* 5, 97.
7. Crair, M.C., and Malenka, R.C. (1995). A critical period for long-term potentiation at thalamocortical synapses. *Nature* 375, 325.

8. Feldman, D.E., Nicoll, R.A., Malenka, R.C., and Isaac, J.T.R. (1998). Long-Term Depression at Thalamocortical Synapses in Developing Rat Somatosensory Cortex. *Neuron* *21*, 347.
9. Hogsden, J.L., and Dringenberg, H.C. (2009). Decline of long-term potentiation (LTP) in the rat auditory cortex in vivo during postnatal life: Involvement of NR2B subunits. *Brain Research* *1283*, 25.
10. Jiang, B., Trevino, M., and Kirkwood, A. (2007). Sequential Development of Long-Term Potentiation and Depression in Different Layers of the Mouse Visual Cortex. *J. Neurosci.* *27*, 9648-9652.
11. Poo, C., and Isaacson, J.S. (2007). An Early Critical Period for Long-Term Plasticity and Structural Modification of Sensory Synapses in Olfactory Cortex. *J. Neurosci.* *27*, 7553-7558.
12. Hanlon, R.T., and Messenger, J.B. (1996). *Cephalopod behaviour* (Cambridge University Press).
13. Dayan, P., and Abbott, L.F. (2001). *Theoretical neuroscience: computational and mathematical modeling of neural systems* (Cambridge: MIT).
14. Shriki, O., Hansel, D., and Sompolinsky, H. (2003). Rate models for conductance-based cortical neuronal networks. *Neural Computation* *15*, 1809-1841.
15. Wilson, H.R., and Cowan, J.D. (1972). Excitatory And Inhibitory Interactions In Localized Populations Of Model Neurons. *Biophysical Journal* *12*, 1-14.